



**HAL**  
open science

## Human Tribbles 3 Protects Nuclear DNA from Cytidine Deamination by APOBEC3A

Marie-Ming Aynaud, Rodolphe Suspène, Pierre-Olivier Vidalain, Bianka Mussil, Denise Guétard, Frédéric Tangy, Simon Wain-Hobson, Jean Pierre Vartanian

► **To cite this version:**

Marie-Ming Aynaud, Rodolphe Suspène, Pierre-Olivier Vidalain, Bianka Mussil, Denise Guétard, et al.. Human Tribbles 3 Protects Nuclear DNA from Cytidine Deamination by APOBEC3A. *Journal of Biological Chemistry*, 2012, 287 (46), pp.39182-39192. 10.1074/jbc.M112.372722 . pasteur-03520008

**HAL Id: pasteur-03520008**

**<https://pasteur.hal.science/pasteur-03520008>**

Submitted on 10 Jan 2022

**HAL** is a multi-disciplinary open access archive for the deposit and dissemination of scientific research documents, whether they are published or not. The documents may come from teaching and research institutions in France or abroad, or from public or private research centers.

L'archive ouverte pluridisciplinaire **HAL**, est destinée au dépôt et à la diffusion de documents scientifiques de niveau recherche, publiés ou non, émanant des établissements d'enseignement et de recherche français ou étrangers, des laboratoires publics ou privés.



Distributed under a Creative Commons Attribution 4.0 International License

# Human Tribbles 3 Protects Nuclear DNA from Cytidine Deamination by APOBEC3A<sup>\*S</sup>

Received for publication, April 18, 2012, and in revised form, September 12, 2012. Published, JBC Papers in Press, September 13, 2012, DOI 10.1074/jbc.M112.372722

Marie-Ming Aynaud<sup>†1</sup>, Rodolphe Suspène<sup>‡2</sup>, Pierre-Olivier Vidalain<sup>§</sup>, Bianka Mussil<sup>‡</sup>, Denise Guétard<sup>‡</sup>, Frédéric Tangy<sup>§</sup>, Simon Wain-Hobson<sup>‡3</sup>, and Jean-Pierre Vartanian<sup>‡</sup>

From the <sup>†</sup>Molecular Retrovirology Unit and <sup>§</sup>Viral Genomic and Vaccination Unit, CNRS URA3015, Institut Pasteur, 28 rue du Dr Roux, F-75724 Paris cedex 15, France

**Background:** APOBEC3A can hyperedit nuclear DNA and generates double-stranded DNA breaks.

**Results:** TRIB3 is an interactor for APOBEC3A and APOBEC3C. TRIB3 is a negative regulator of APOBEC3A.

**Conclusion:** Through its control of APOBEC3A, TRIB3 is another guardian of genome integrity.

**Significance:** TRIB3 is part of protein network that involves cell cycle control, cell survival, DNA repair, and genome stability.

The human polydeoxynucleotide cytidine deaminases APOBEC3A, APOBEC3C, and APOBEC3H are capable of mutating viral DNA in the nucleus, whereas APOBEC3A alone efficiently edits nuclear DNA. Deamination is rapidly followed by excision of uracil residues and can lead to double-stranded breaks. It is not known to which protein networks these DNA mutators belong. Using a yeast two-hybrid screen, we identified the human homolog of *Drosophila* Tribbles 3, TRIB3, as an interactor for APOBEC3A and APOBEC3C. The interaction was confirmed by co-affinity purification. Co-transfection of APOBEC3A with a TRIB3 expression vector reduced nuclear DNA editing whereas siRNA knockdown of TRIB3 increased the levels of nuclear DNA editing, indicating that TRIB3 functioned as a repressor of A3A. It also repressed A3A-associated  $\gamma$ H2AX positive double-stranded breaks. The interaction results in degradation of A3A in a proteasome-independent manner. TRIB3 has been linked to cancer and via its own interactors and links the A3A DNA mutators to the Rb-BRCA1-ATM network. TRIB3 emerges as an important guardian of genome integrity.

The human genome encodes eight cytidine deaminases (A1, A3A–C, A3F–H, AID) capable of mutating DNA of which AID, responsible for immunoglobulin class switch recombination and somatic hypermutation, is perhaps the most widely known example (1, 2). Several of the APOBEC3 (A3) cytidine deaminases can target retroviral cDNA intermediates, notably human immunodeficiency virus (HIV), the result being DNA peppered with cytidine to uridine mutations (3–7). Indeed, APOBEC3F and APOBEC3G (A3F and A3G) proved such a barrier to HIV that it evolved an antagonist encoded by the viral gene, *vif*

(8–10). Recently, it was shown that A3D impacted HIV-1 replication (11, 12). Hepatitis B virus (HBV),<sup>4</sup> a nonclassical retrovirus, is also susceptible to restriction by A3 enzymes, particularly in late stage disease, with A3G and probably A3C being the major players (13–17). Unlike HIV, HBV does not encode an A3 antagonist.

DNA viral genomes too can be edited, notably human papillomavirus types 1a and 16 (18), as well as herpes simplex virus type 1 (HSV-1), Epstein-Barr virus (19), and transfusion transmitted virus (20). For human papillomaviruses the restricting molecules are A3A, A3C, and A3H whereas for HSV-1 only A3C edits efficiently. Not surprisingly, the single-stranded (ss) DNA genomes of parvoviruses are vulnerable to A3 editing (21, 22). As such, the A3 enzymes constitute a set of viral restriction factors. This notion is supported by the finding that several A3 genes, notably A3A and A3G, are up-regulated by type I and II interferons (23–26). As all these DNA viruses replicate in the nucleus, the intriguing question as to how A3 enzymes in the nucleus distinguish between viral and host nuclear DNA (nuDNA), if at all, comes to the fore.

Recent work has shown that A3 restriction of viral genomes is only part of the picture (26–28). Human mitochondrial DNA (mtDNA) can be hyperedited *in vivo* and in tissue culture experiments involving A3 enzymes (28). Editing occurred at relatively low levels in the cytoplasm. At least five A3 enzymes were involved, although as A3C is invariably the most abundant A3 enzyme expressed it is likely that much of the editing could be attributed to it (28). By contrast, A3A is singular in that it can hyperedit nuDNA outside of any microbial context (28). Observed levels of both mtDNA and nuDNA editing are rate-limited by uracil DNA-glycosylase (UNG) for, in the absence of UNG, far more hyperedited mt and nuDNA could be detected (28). Apart from mutating DNA, A3A appears to generate double-stranded DNA breaks (DSBs) thus reflecting the two attributes of AID, *i.e.* class switch recombination and somatic hypermutation (27, 29). These activities are carefully con-

\* This work was supported by grants from Institut Pasteur and the CNRS. The Molecular Retrovirology Unit is équipe labellisé par la Ligue pour la Recherche contre le Cancer.

<sup>S</sup> This article contains supplemental supplemental Figs. S1–S4.

<sup>1</sup> Supported by a graduate fellowship from la Ligue pour la Recherche contre le Cancer.

<sup>2</sup> Supported by a postdoctoral fellowship from l'Association pour la Recherche contre le Cancer.

<sup>3</sup> To whom correspondence should be addressed: Molecular Retrovirology Unit, Institut Pasteur, CNRS URA3015, 28 rue du Dr Roux, F-75724 Paris cedex 15, France. Tel.: 33-1-45-68-88-21; Fax: 33-1-45-68-88-74; E-mail: simon.wain-hobson@pasteur.fr.

This is an Open Access article under the [CC BY](#) license.

<sup>4</sup> The abbreviations used are: HBV, hepatitis B virus; Bis-Tris, bis(2-hydroxyethyl)iminotris(hydroxymethyl)methane; DSB, double-stranded break; Gal4-BD, Gal4-binding domain; mtDNA, mitochondrial DNA; NLS, nuclear localization signal; nuDNA, nuclear DNA; PBMC, peripheral blood mononuclear cell; TRIB3, Tribbles 3; UNG, uracil DNA-glycosylase.

trolled, and AID interacts with a number of proteins to achieve specificity (30, 31). However, AID can edit nuDNA outside of the rearranged IgV locus and has been implicated in the development of cancers (32). Ectopic expression of *AICDA* has been noted in a number of cancers and tissues unrelated to germinal center B cells (33, 34). Indeed, *AICDA* transgenic mice develop cancers, the type depending on the cell tropism of promoter used (35, 36). Similar findings were made for transgenic mice bearing the eponymous *APOBEC1* gene (37).

Using the AID paradigm, it is probable that the ssDNA A3 mutators interact with numerous proteins. This is indeed the case for A3G, which is particularly present in cytoplasmic P bodies (38). Interactors for the other APOBEC3 deaminases have not yet been reported. Given our interest in the restriction of DNA viruses replicating in the nucleus and the finding that A3A can edit nuDNA, we set out to identify interactors for the A3A, A3C, and A3H deaminases, all of which have cytoplasmic and nuclear localizations. We found that A3A and A3C interacted with the human homolog to the *Drosophila* protein, Tribbles 3 (TRIB3) (39). Although it shares homology to serine/threonine kinases such as PIM1, it is actually a pseudokinase (40). TRIB3 is an inhibitor of AKT, a prosurvival kinase (41), is implicated in diabetes (41), and is part of G<sub>1</sub>/S and G<sub>2</sub>/M checkpoint control (42, 43). siRNA knockdown of *TRIB3* resulted in increased A3A editing of nuDNA whereas overexpression reduced editing, indicating that it was a negative regulator of A3A. TRIB3 emerges as another guardian of genome integrity.

## EXPERIMENTAL PROCEDURES

**Reagents**—siTRIB1 (sc-77704), siTRIB2 (sc-94644), siTRIB3 (sc-44426), and control siRNAs (sc-44237) were from Santa Cruz Biotechnology. Epoxomicin and bafilomycin were from Sigma. TRIB3 shRNA and control shRNA lentiviral particles were from Santa Cruz Biotechnology. A3A antibodies (SAB4500753) were from Sigma. Type I IFN- $\alpha$ A (6.8 $\times$ 10<sup>8</sup> units/mg) were from PBL Biomedical Laboratories. The A3A constructs have been described previously (28). The TRIB1 and TRIB2 constructs were recloned into pCI-neo-3 $\times$ FLAG vector. The precise amino acid sequences of the 3 $\times$ FLAG-tagged TRIB constructs as well as the A3A-NLS construct are given in supplemental Fig. S1. The HEK-293T-UGI cell line has been described (26).

**Cells**—Approximately 450,000 HeLa cells, HEK-293T, and HEK-293T-UGI were seeded in 6-well plates and transfected 24–48 h later by 2  $\mu$ g of total plasmid using JetPrime (Polyplus Transfection<sup>TM</sup>). 100,000 U937 cells were stimulated by IFN I $\alpha$ A (1000 units/ml) and were transduced by TRIB3 shRNA or control shRNA lentiviral particles (Santa Cruz Biotechnology). After 48 h, total DNA was extracted. For imaging, 25,000 HeLa cells were seeded in Lapteck and transfected 36 h later by 100 ng of total plasmid using FuGENE HD Transfection Reagent (Roche Applied Science).

**Plasmids**—cDNAs encoding for APOBEC3A, APOBEC3C, APOBEC3G, APOBEC3H, TRIB1, TRIB2, or TRIB3 were amplified by standard PCR (*Taq* Platinum; Invitrogen) and cloned by *in vitro* recombination in pDONR207 using Gateway technology (Invitrogen). PCR primers displayed 20–30 specific nucleotides matching ORF extremities so that their *T<sub>m</sub>* is close

to 60 °C. The 5' ends of Gateway forward primers were fused to attB1.1 recombination sequence 5'-GGGGACAACCTTGTACAAAAAGTTGGCATG-3', whereas reverse primers were fused to attB2.1 recombination sequence 5'-GGGGACAACCTTGTACAAGAAAGTTGGTTA-3'. Recombination of PCR products into pDONR207 was performed following the manufacturer's recommendation (BP cloning reaction; Invitrogen). All constructs were transformed and amplified in *Escherichia coli* DH5 $\alpha$  strain.

**Yeast Two-hybrid Screen**—Yeast culture media were prepared as described previously (44). A3A and A3C coding sequences were transferred by *in vitro* recombination (LR cloning reaction, Gateway technology) from pDONR207 into yeast two-hybrid vector pDEST32 (Invitrogen) to be expressed in fusion downstream of Gal4 binding domain (Gal4-BD). Bait constructs were transformed into AH109 yeast strain (Clontech) using a standard lithium acetate procedure. Spontaneous transactivation of the *HIS3* reporter gene was not observed in yeast cells expressing Gal4-BD-APOBEC3C. Consequently, the screen was performed on a synthetic medium lacking histidine (–His medium) and not supplemented with 3-amino-1,2,4-triazole. A mating strategy was used for screening a human spleen cDNA library cloned in the Gal4-AD pPC86 vector (Invitrogen) and previously established into the Y187 yeast strain (Clontech). After 6 days of culture on –His selective medium, [His<sup>+</sup>] colonies were selected and purified over 3 weeks by culture on selective medium to eliminate false positives. AD-cDNAs were amplified by PCR from zymolase-treated yeast colonies using primers that hybridize within the pPC86 regions flanking cDNA inserts. PCR products were sequenced, and cellular interactors were identified by multiparallel BLAST analysis.

**Co-affinity Purification**—To perform co-affinity purification experiments, cloned ORFs were transferred from pDONR207 to pDEST27 expression vector (Invitrogen) to achieve GST fusion, and to pCI-neo-3 $\times$ FLAG vector (45) for 3 $\times$ FLAG fusion. Tagged proteins were expressed in human HEK-293T cells maintained in Dulbecco's modified Eagle's medium (DMEM; Invitrogen) containing 10% fetal bovine serum, penicillin, and streptomycin at 37 °C and 5% CO<sub>2</sub>. Cell transfections were achieved with JetPrime reagent following the manufacturer's recommendations. Briefly, 5 $\times$ 10<sup>5</sup> HEK-293T cells were dispensed in each well of a 6-well plate and transfected 24 h later with 300 ng of the GST constructs and 100 ng of the 3 $\times$ FLAG constructs. Two days after transfection, HEK-293T cells were washed in phosphate-buffered saline (PBS) and then resuspended in lysis buffer (0.5% Nonidet P-40, 20 mM Tris-HCl, pH 7.4, 120 mM NaCl, and 1 mM EDTA) supplemented with Complete Protease Inhibitor Mixture (Roche Applied Science). Cell lysates were incubated on ice for 20 min and then clarified by centrifugation at 14,000  $\times$  g for 30 min. For pulldown analysis, 400  $\mu$ g of protein extracts were incubated for 1 h at 4 °C with 25  $\mu$ l of glutathione-Sepharose beads (Amersham Biosciences) to purify GST-tagged proteins. Beads were then washed three times in ice-cold lysis buffer, and proteins were recovered by boiling in ice-cold lysis loading buffer (Invitrogen). Purified complexes and protein extracts were resolved by SDS-polyacrylamide gel electrophoresis (SDS-PAGE) on 4–12% NuPAGE Bis-Tris gels with MOPS running buffer (Invitrogen), and

### Tribbles 3 Protects Nuclear DNA from APOBEC3A

transferred to a nitrocellulose membrane. 3×FLAG and GST-tagged proteins were detected using standard immunoblotting techniques. Membranes were blotted with a mouse monoclonal HRP conjugated anti-3×FLAG antibody (M2; Sigma) or a rabbit polyclonal anti-GST antibody (Sigma). Secondary anti-rabbit HRP-conjugated antibody was from Amersham Biosciences.

To detect the physiological interaction between A3A and TRIB3, protein extracts were precleared for 1 h with protein G-Sepharose Fast Flow (Sigma). The supernatant without the sticky protein was incubated for 1 h with TRIB3 antibody (Santa Cruz Biotechnology) or with an antibody with the same isotype of TRIB3 (IgG<sub>2b</sub>) or without antibody. The complex was incubated for 1 h in presence of protein G-Sepharose Fast Flow. Western blotting was performed in presence of a rabbit anti-A3A antibody at 1/1000 dilution (Sigma) or a mouse anti-TRIB3 antibody at 1/1000 dilution (Santa Cruz Biotechnology) followed by a secondary antibody anti-rabbit or anti-mouse at 1/10,000 (GE Healthcare).

**PCR and 3D-PCR**—For amplification of human *CMYC*, the first-round reaction parameters were 95 °C for 5 min followed by 42 cycles (95 °C for 1 min, 57 °C for 45 s, and 72 °C for 1 min) and finally 10 min at 72 °C. Second-round three-dimensional PCR were performed using the equivalent of 0.5 μg of the first-round reaction as input using Eppendorf gradient Mastercycler S. The reaction parameters were 91–95 °C for 5 min followed by 42 cycles (91–95 °C for 1 min, 57 °C for 1 min, and 72 °C for 2 min), and finally 10 min at 72 °C. All DNAs were extracted using the Epicenter kit. All amplifications were performed using first-round standard PCR followed by nested three-dimensional PCR. PCR was performed with 2.5 units of *Taq* (Bioline) DNA polymerase per reaction. PCR products were cloned using the TOPO vector, and sequencing was outsourced to GATC. The human *CMYC* primers have been described (28).

**Confocal Microscopy**—After PBS washing, cell were fixed in 50/50 methanol/acetone for 20 min at room temperature. The anti-V5 antibody (Invitrogen) and anti-3×FLAG antibody (Sigma) were incubated at 1/200 for 1 h at room temperature (Sigma) followed by incubation with fluorescein-conjugated secondary antibody for 1 h at room temperature. Slides were mounted with Vectashield-DAPI. Confocal Imaging was performed using a Zeiss AxiomagerZ2 LSM700. HCX PL APOS63 × 1.4 OIL optics was used.

**Western Blotting**—Total protein was recovered 24 h after transfection. Western blot analysis was carried out according to standard procedures by using a mouse monoclonal specific for the V5 epitope (Invitrogen) applied for 1 h. After incubation with an anti-mouse IgG horseradish peroxidase-coupled secondary antibody (Amersham Biosciences), the membrane was subjected to detection by enhanced chemiluminescence (Pierce).

**PBMC, CD4, and Neutrophil Purification**—Ficoll-purified peripheral blood mononuclear cells (PBMCs) were stimulated with phytohemagglutinin (Sigma), IL2 (Sigma) and IFNα (PBL, Biomedical Laboratories). CD4 isolation has been performed with antibody-coated magnetic beads (Miltenyl Biotec). Human neutrophils were isolated from peripheral blood of

healthy donors using the human neutrophils enrichment kit (negative selection EasySep Kit), according to the manufacturer's instructions (StemCell Technologies).

**Transcriptomes**—For the cirrhosis samples the methods have been described (17). For the cell lines and PBMCs, all extractions were performed with RNA EXTRACT RNeasy® Plus Mini Kit (Qiagen). The APOBEC3 primers and probes have been described (25). The TRIB3 oligonucleotides were designed using Roche Applied Science probe finder version 2.43: TRIB3, 5'-GTCTTCGCTGACCGTGAGA; TRIB3, 3'-CAGTCAG-CAGCGAGGAGTC; probe 67, TGCTGGAG.

**FACS Analysis of Double-stranded Breaks**—24 h after transfection, cells were washed with PBS, fixed in 2–4% ice-cold paraformaldehyde (Electron Microscopy Sciences) for 10 min, and permeabilized in 90% ice-cold methanol (Sigma) for 30 min. After washing with PBS, cells were incubated with 1:200 diluted mouse anti-V5 antibody (Invitrogen) for 1 h followed by incubation with 1:500 diluted Alexa Fluor 633 F(ab')<sub>2</sub> fragment of goat anti-mouse IgG (H+L) (Invitrogen) for 45 min. DNA double-stranded breaks were analyzed by staining for 1 h with 1:50 diluted Alexa Fluor 488-conjugated rabbit monoclonal anti-γH2AX (20E3) antibody (Cell Signaling). All incubation steps were performed on ice. 10<sup>4</sup> cells were analyzed on FACSCalibur using CellQuest Pro (BD Biosciences, version 5.2) and FlowJo software (Tree Star, Inc., version 8.7.1).

## RESULTS

**Tribbles Homolog 3 Is an Interactor for A3A and A3C**—Complete A3A, A3C, and A3H cDNA coding sequences were cloned in a yeast vector to be used as bait in the two-hybrid system. A3 ORFs were expressed as fusion proteins downstream of the Gal4-BD. We failed to obtain yeast colonies with Gal4-BD-A3A, suggesting that A3A is toxic in yeast. This interpretation is supported by viable expression of the A3A<sub>C101S</sub> catalytic mutant in the same system. By contrast, Gal4-BD-A3C and Gal4-BD-A3H constructs did not interfere with yeast growth and were used as bait to screen a human cDNA library made from human spleen (Invitrogen) for partners. A3H failed to capture any prey proteins. By contrast, numerous yeast colonies were obtained on selective medium with the Gal4-BD-A3C construct, and interacting prey proteins were identified by PCR, sequencing, and multiparallel BLAST analysis. From among 2·10<sup>7</sup> colonies screened from a library made from human spleen (Invitrogen), we recovered 4 hits for the human *TRIB3* first identified for *Drosophila*. All hits were full-length cDNAs showing two known synonymous polymorphisms at codons 111 and 320. In more than 250 screens performed using different bait proteins of either viral or human origin, this is the first time we have identified *TRIB3*.

To confirm the interaction, we performed co-affinity purification experiments (GST pull-down). HEK-293T cells were co-transfected by a 5' 3×FLAG-TRIB3 construct along with GST-A3A, GST-A3C, GST-A3H, and GST-A3G as negative control. As can be seen from Fig. 1A, A3C interacted strongly with TRIB3 whereas for A3A the interaction was weaker. Human A3H and the A3G negative control failed to pull down TRIB3. To confirm the specificity of the A3A and A3C co-affinity purification, we explored the possible interaction with either of the

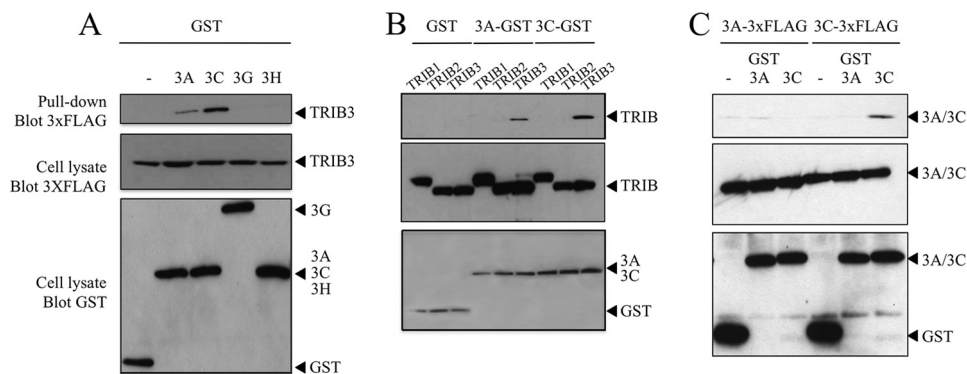


FIGURE 1. **APOBEC3A and 3C interact with human TRIB3 protein.** *A*, GST pull-downs were followed by Western blotting with antibodies to 3×FLAG. Below are the TRIB3 and APOBEC3 controls. *B*, interaction was specific for TRIB3 compared with the paralogous human proteins TRIB1 and TRIB2 (see supplemental Fig. S1A for sequence comparisons). *C*, APOBEC3C but not APOBEC3A can form multimers.

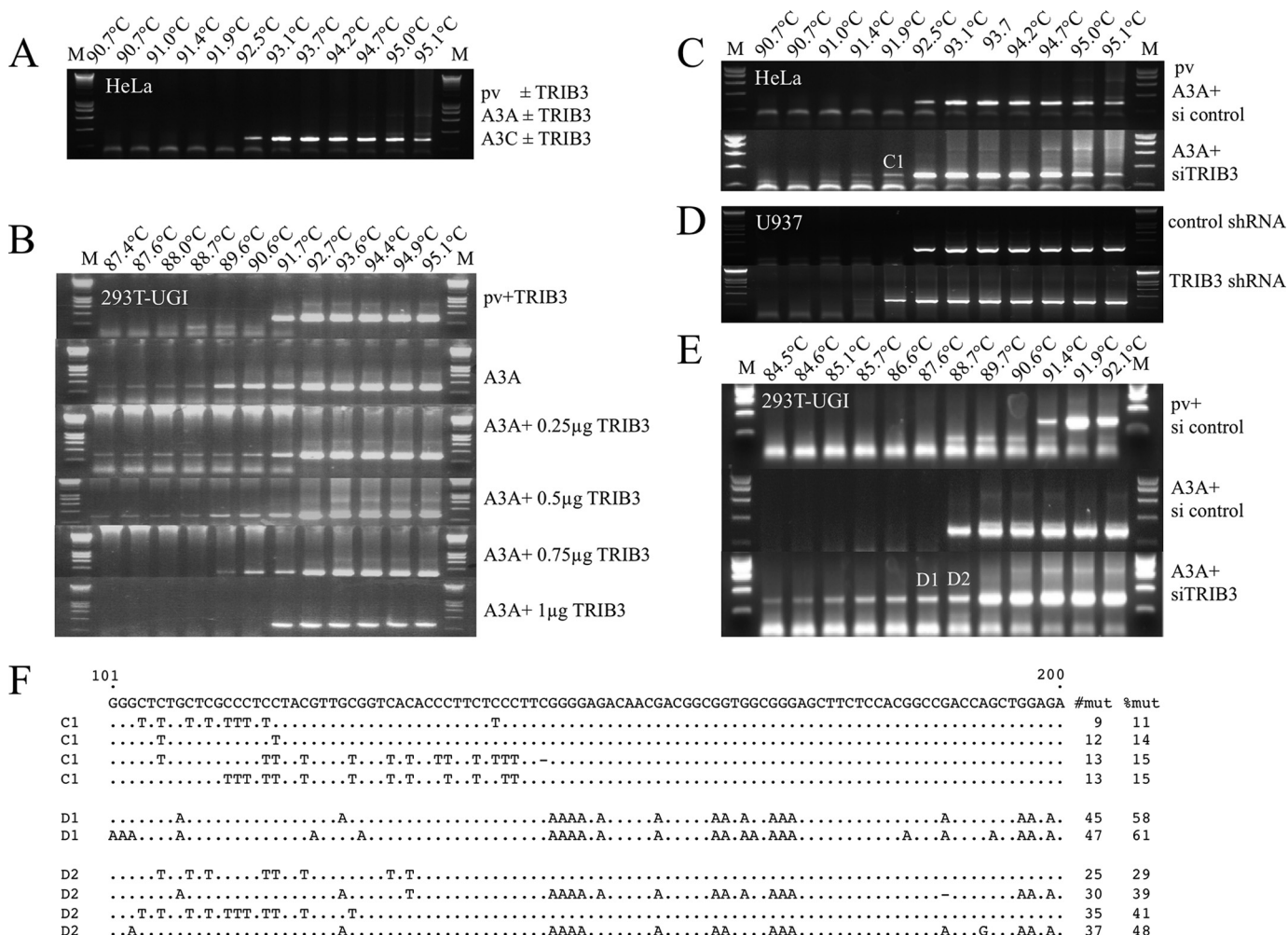


FIGURE 2. **TRIB3 protects whereas TRIB3 siRNA knockdown increases A3A deamination of nuDNA.** *A*, no apparent deamination of *CMYC* DNA by A3A or A3C ± TRIB3 in HeLa cells was due to rate-limiting UNG degradation. *B*, in HEK-293T-UGI cells TRIB3 protects nuDNA from editing by A3A in a dose-response manner. DNA concentrations were 2 μg throughout and were compensated for by plasmid vector. *C*, co-transfection of A3A with 1 μg of TRIB3 siRNA knockdown only results in recovery of hyperedited *CMYC* DNA in HeLa cells. *D*, transduction of IFNαA stimulated U937 cells with TRIB3 shRNA or control shRNA lentiviral particles. *E*, co-transfection of A3A with 1 μg of TRIB3 siRNA knockdown only results in recovery of enhanced hyperediting of *CMYC* DNA in 293T-UGI cells. *F*, a collection of hyperedited *CMYC* sequences was recovered from samples C1, D1, and D2 (*C* and *E*). Only differences are shown for 100 bases of a total of 241 bp. To the right are the number mutations per sequence and the percentages of Cs or Gs (Cs on opposite strand) edited.

other two human *Tribbles* homologs, TRIB1 and TRIB2 which show ~46 and 48% amino acid identity with TRIB3 (supplemental Fig. S1A). No interaction was found with either protein confirming the specificity of the A3A/TRIB3 and A3C/TRIB3

interactions (Fig. 1B). Although TRIB1 is nuclear, no co-localization with A3A was observed whereas for TRIB2 a nonspecific co-localization was noted and follows on from the fact that both TRIB2 and A3A are partitioned between the nucleus and

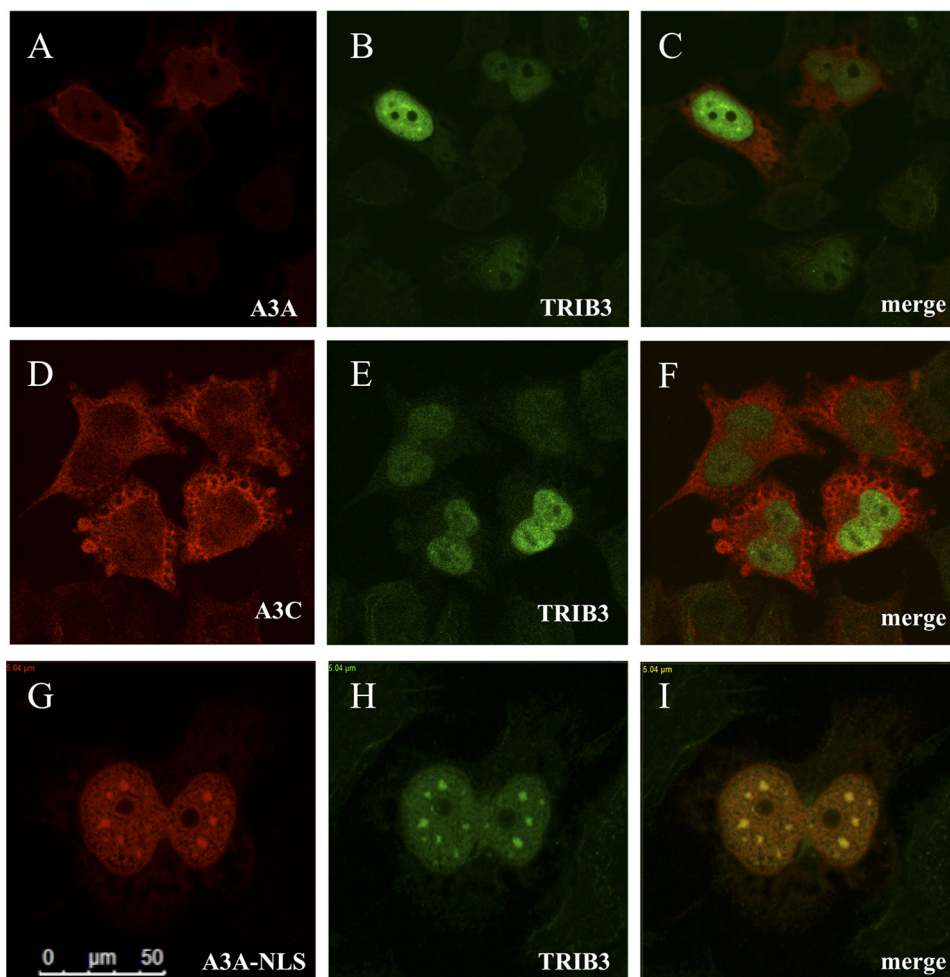


FIGURE 3. **Cell localization of the A3A and TRIB3.** A–C, confocal microscopy yielding scant evidence of cytoplasmic and slightly nuclear A3A-V5 co-localizing with a nuclear 3×FLAG-TRIB3 in HeLa cells 36 h after transfection. D–F, A3C, TRIB3, and merge. G–I, addition of the SV40 NLS (residues PPKKKRKY) to the carboxyl terminus of A3A co-localization with TRIB3 is readily observed.

cytoplasm (supplemental Fig. S2A). As some APOBEC3 proteins homo- and heterodimerize, notably A3B, A3F, and A3G (2, 9), we tested the possibility that A3A and A3C could form dimers. In the same co-affinity purification format, A3C formed homodimers but not heterodimers with A3A, whereas A3A failed to do either (Fig. 1C). It is possible that the apparent stronger interaction between TRIB3 and A3C might reflect greater avidity, given A3C dimer formation. To see whether A3C affect the A3A/TRIB3 interaction, HEK-293T cells were transfected with A3A-GST (300 ng) and 3×FLAG-TRIB3 (100 ng) and with an increasing amount of 3×FLAG-A3C (50, 200, 800 ng). After 24 h, cells were lysed with a radioimmune precipitation assay buffer, and total proteins were extracted. We proceeded to a co-purification affinity and observed that an increased concentration of A3C did not affect the A3A/TRIB3 interaction (supplemental Fig. S3A).

**Tribbles 3 Inhibits A3A Editing of Nuclear DNA**—HeLa cells were co-transfected with TRIB3 and V5-tagged A3 expression plasmids with recovery of cytidine deamination of *CMYC* DNA as readout (28). Normally transfection with A3A alone followed by 3D-PCR (46) fails to recover hyperedited *CMYC* from HeLa cell DNA (28). Co-transfection with TRIB3 did not change the situation (Fig. 2A). Detection of *CMYC* editing represents a

dynamic between A3A editing and DNA catabolism by a UNG initiated pathway, the latter being rate-limiting. HEK-293T-UGI cells, which constitutively express the UNG inhibitor, UGI (47), allow detection of edited *CMYC* DNA following A3A transfection (28). Accordingly, HEK-293T-UGI cells were co-transfected by A3 expression plasmids with and without TRIB3. Now, TRIB3 expression proved to inhibit A3A editing of *CMYC* in a dose-dependent manner (Fig. 2B). As previously noted, transfection with A3C, A3H, and A3G had no impact on *CMYC* editing, a finding that was not altered either by co-transfection with TRIB3 or with TRIB1 or TRIB2 (supplemental Fig. S2, B and C). Given that two-hybrid screens pick up a subset of protein interactors, the remaining APOBEC3 enzymes were tested, notably A3B and A3F with and without all three TRIB constructs (supplemental Figs. S2, B and C). Again, no evidence of *CMYC* editing was identified by the nested PCR/3D-PCR protocol.

If TRIB3 was restricting A3A activity then *TRIB3* siRNA knockdown should enhance A3A editing of *CMYC*. This is, indeed the case for HeLa cells (Fig. 2, C and F), or for IFN I $\alpha$ -stimulated U937 cells transduced with *TRIB3* shRNA or control shRNA lentiviral particles (Fig. 2D). Hyperedited *CMYC* was obtained at restrictive temperature of 91.4 °C and

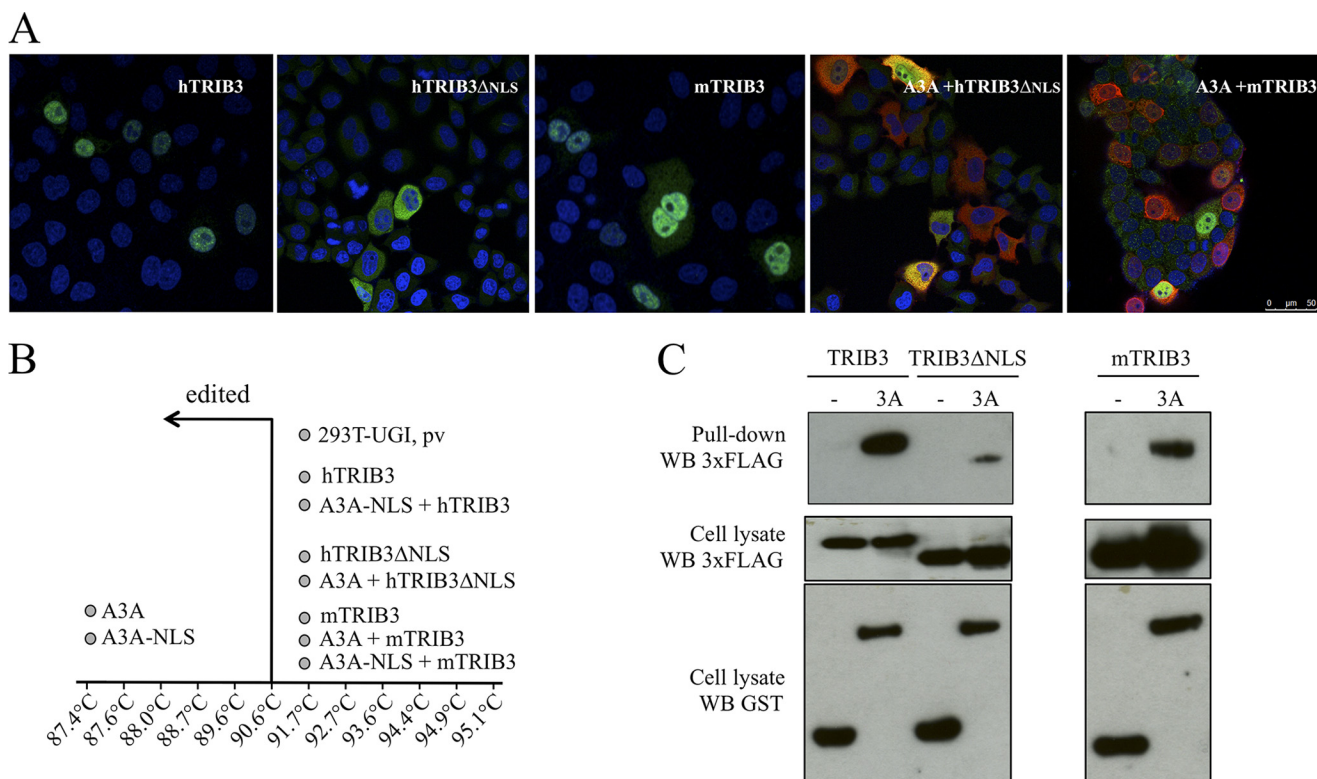


**FIGURE 4. The A3A interaction involves the amino terminus of TRIB3.** *A*, immunofluorescence of TRIB3, its cytoplasmic  $\Delta$ NLS derivative, and the murine homolog, mTRIB3. *B*, *CMYC* editing by A3A, A3A-NLS, and modulation by an amino-terminal 36-residue deletion of hTRIB3. *C*, GST pull-down analyses for the A3A+TRIB3, +TRIB3 $\Delta$ NLS, and +mTRIB3 constructs. *WB*, Western blot.

91.9 °C in the presence of TRIB3 shRNA (Fig. 2*D*). For the HEK-293T-UGI cell line co-transfection of A3A+siTRIB3 allowed recovery of hyperedited *CMYC* DNA down to 84.5 °C, the lowest *CMYC* 3D-PCR denaturation temperature from any experimental conditions identified to date (Fig. 2, *E* and *F*). Efficiency of TRIB3 siRNA was performed and presented in supplemental Fig. S3*H*. A collection of hyperedited *CMYC* sequences recovered from samples C1, D1, and D2 is presented in Fig. 2*F*. This result is worth emphasizing for it is the first time we have recovered edited *CMYC* DNA without recourse to either *UNG* knockdown, or *UNG*<sup>-/-</sup> cell lines (28). *TRIB3* siRNA knockdown failed to reveal any A3C or A3H-associated nuDNA editing (supplemental Fig. S2, *B* and *C*) confirming our previous negative findings even with UGI (28). Indeed, co-transfection of HEK-293T-UGI cells by A3C or A3H along with siRNAs for *TRIB3*, *TRIB2* or *TRIB1* failed to yield hyperedited *CMYC* DNA, emphasizing the singularity of the A3A interaction with *TRIB3* (supplemental Fig. S2*C*).

**Cell Localization of A3A, A3C, and TRIB3**—The localization of overexpressed A3A-V5 and A3C-V5 in HeLa cells is mainly cytoplasmic with a nuclear component, whereas 3 $\times$ FLAG-*TRIB3* is exclusively nuclear (supplemental Fig. S4*B*) in keeping with published reports (21, 27, 48). Co-transfection of A3A+*TRIB3* showed neither substantial relocalization of A3A to the nucleus nor strong co-localization within the nucleus, indicating that *TRIB3* is not transporting A3A to the nucleus (Fig. 3, *A–C*). The same was true for A3C (Fig. 3, *D–F*). To force the system, we tagged A3A with the SV40 TAg nuclear localization signal (NLS, residues PPKKKRKV). Now, most A3A-

NLS-V5 was located in the nucleus and co-localized with 3 $\times$ FLAG-*TRIB3* in a punctuate distribution (Fig. 3, *G–I*). As expected, A3A-NLS hyperedited *CMYC* in the HEK-293T-UGI cell line to a similar degree compared with A3A, whereas co-transfection with *TRIB3* reduced the degree of editing (Fig. 4*B* and supplemental Fig. S4*A*).

**The TRIB3 Amino Terminus Modulates the Interaction with A3A**—*TRIB3* encodes numerous basic residues at its amino terminus that resemble a bipartite nuclear localization signal (supplemental Fig. S1*B*). If correct, we reasoned that a 3 $\times$ FLAG-*TRIB3* $\Delta$ NLS construct should no longer be capable of inhibiting A3A deamination of nuDNA. Deletion of the first 36 residues yielded a protein that was strictly cytoplasmic (Fig. 4*A*). Co-transfection of HEK-293T-UGI cells with A3A showed that the 3 $\times$ FLAG-*TRIB3* $\Delta$ NLS abrogated A3A editing on nuDNA (Fig. 4*B* and supplemental Fig. S4*A*), an experiment performed independently four times with the same result suggesting that A3A was functionally restricted by 3 $\times$ FLAG-*TRIB3* $\Delta$ NLS. In agreement with this, GST pull-down experiments revealed a greatly reduced interaction between the two partners (Fig. 4*C*). Murine *TRIB3* shows ~74% overall homology to its human *TRIB3* counterpart (supplemental Fig. S1*B*) and is also exclusively nuclear (Fig. 4*A*). Interestingly, co-transfection of HEK-293T-UGI cells with m*TRIB3* and A3A abrogated A3A editing of *CMYC* DNA like its human counterpart (Fig. 4*B* and supplemental Fig. S4*A*). Finally, by co-affinity purification, we have also demonstrated the interaction between A3A and m*TRIB3* (Fig. 4*C*).

## Tribbles 3 Protects Nuclear DNA from APOBEC3A

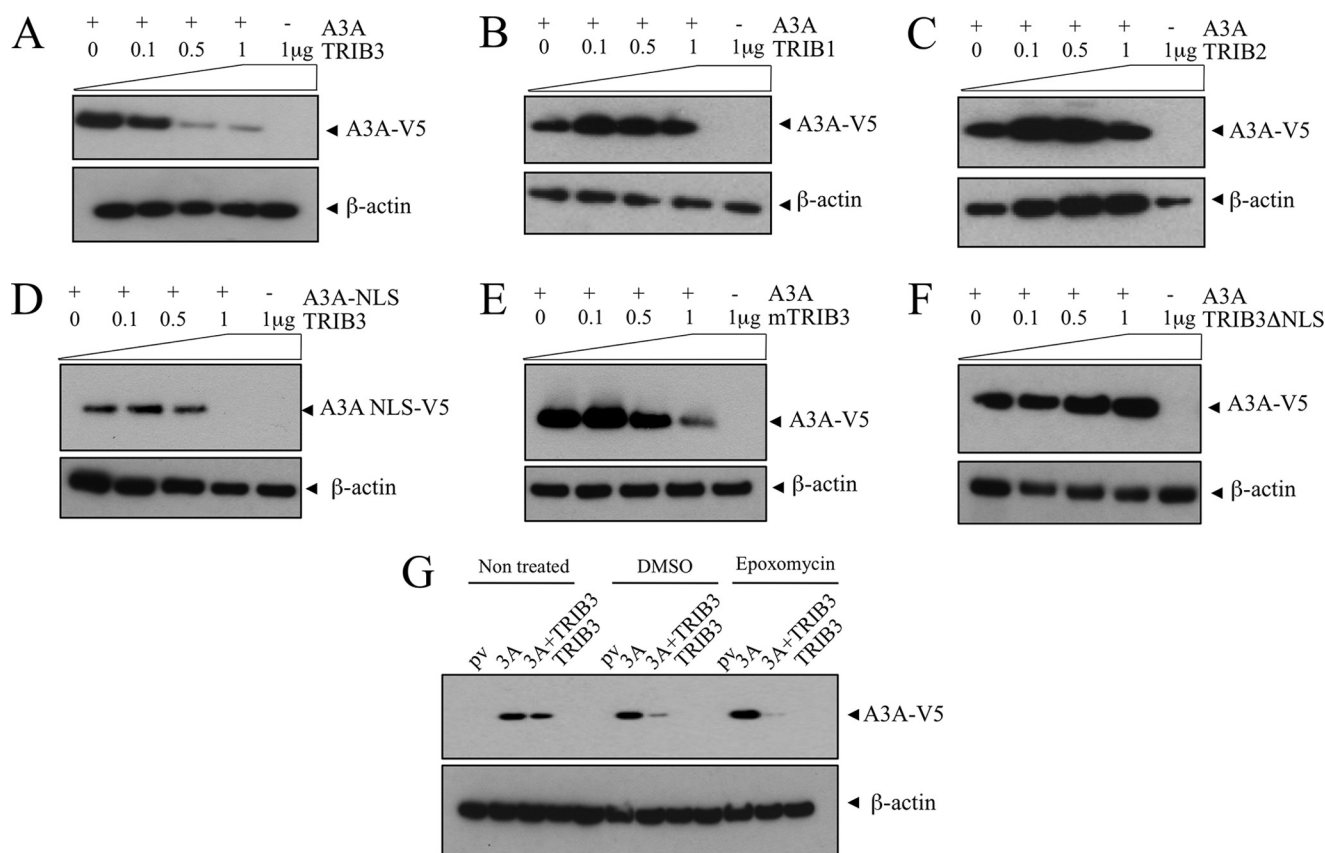


**FIGURE 5. TRIB3 interaction with A3A results in lower steady-state levels.** *A*, 293T cells were transfected by A3A, and increasing concentrations of TRIB3 and steady-state levels of A3A were determined by Western blotting at 24 h. The  $\beta$ -actin loading controls are shown below. *B* and *C*, TRIB1 and TRIB2 do not degrade A3A. *D*, the A3A-NLS construct is similarly degraded. *E*, mTRIB3 is capable of degrading hA3A. *F*, by contrast, deletion of the amino-terminal 36 residues of TRIB3 which include a NLS abrogates A3A degradation. *G*, epoxomycin treatment of 293T cells fails to abrogate A3A degradation by TRIB3.

*Tribbles 3 Reduces Steady-state Levels of A3A*—Clearly TRIB3 and A3A interact but apparently do not co-localize extensively. The amino-terminal pseudo-NADPH binding domain of TRIB3 is proline-rich (19/143, 13% versus carboxyl-terminal 15/215, 7%) which is reminiscent of some highly labile proteins. Indeed, mouse TRIB3 has an extraordinarily short half-life compared with other mouse proteins (49). To see whether TRIB3 expression had any impact on A3A protein levels, HEK-293T cells were co-transfected by V5-tagged A3A and increasing amounts of 3 $\times$ FLAG-TRIB3. A dose-dependent reduction of A3A steady-state levels was noted whereby at approximately equimolar plasmid concentrations A3A was reduced compared with A3A alone (Fig. 5*A*). This destabilization was specific to TRIB3 compared with TRIB1 and TRIB2 taken as controls (Fig. 5, *B* and *C*). The same experiment was performed with A3C with increased amounts of 3 $\times$ FLAG-TRIB3 (0, 0.1, 0.5, 1  $\mu$ g). Similarly to A3A, a dose-dependent reduction of A3C steady-state levels was noted and was specific to TRIB3 compared with TRIB1 and TRIB2 (supplemental Fig. S3, *B–D*).

It is worth noting that this situation (1  $\mu$ g of each plasmid) corresponds to that in Fig. 3, *A–C*, where there was little co-localization of A3A and TRIB3. The same phenomenon occurs for the A3A-NLS construct (Fig. 5*D*), and to a lesser degree for mouse TRIB3 (Fig. 5*E*). However, with deletion of the TRIB3 NLS motif, A3A degradation ceased (Fig. 5*F*). Treatment of

HEK-293T cells with 10  $\mu$ M epoxomycin, a proteasome inhibitor, resulted in more V5-tagged A3A as previously noted (Fig. 5*G*) (50). By contrast, A3A levels decreased when co-expressed with TRIB3, indicating that the A3A-TRIB3 complex is not degraded by the proteasome (Fig. 5*G*), the same phenomenon was observed with A3C-TRIB3 (supplemental Fig. S3*E*). Moreover treatment with 100 nM bafilomycin, a specific inhibitor of vacuolar-type H<sup>+</sup>-ATPase, failed to abrogate A3A or A3C degradation by TRIB3 (supplemental Fig. S3*F*).

*TRIB3 Protects the Cell against A3A-induced Double-stranded DNA Breaks*—Cytidine deamination of DNA can also result in DSBs and follows on from UNG excision of uracil bases and subsequent APE1 cleavage of the DNA backbone at abasic sites (29, 51). This is the case for AID and more recently A3A (27, 52, 53). The  $\gamma$ -phosphorylated form of H2AX is an excellent marker for DSBs (54). As can be seen from Fig. 6, transfection of HeLa cells by A3A resulted in numerous DSBs as evidenced by  $\gamma$ H2AX as a function of A3A-V5-positive cells. By contrast, co-transfection of A3A with TRIB3 resulted in lower numbers of  $\gamma$ H2AX-positive cells and then with lower mean  $\gamma$ H2AX intensity. Overexpression of the A3A<sub>C101S</sub> catalytic mutant, TRIB3 alone, APOBEC2, devoid of any cytidine deaminase activity, or the vector control failed to induce DSBs (Fig. 6*B*). The greater the ratio of TRIB3 to A3A, the smaller the fraction of DSBs. That A3C did not generate DSBs is consistent with its failure to deaminate nuDNA efficiently (28 and Fig. 6*B*).

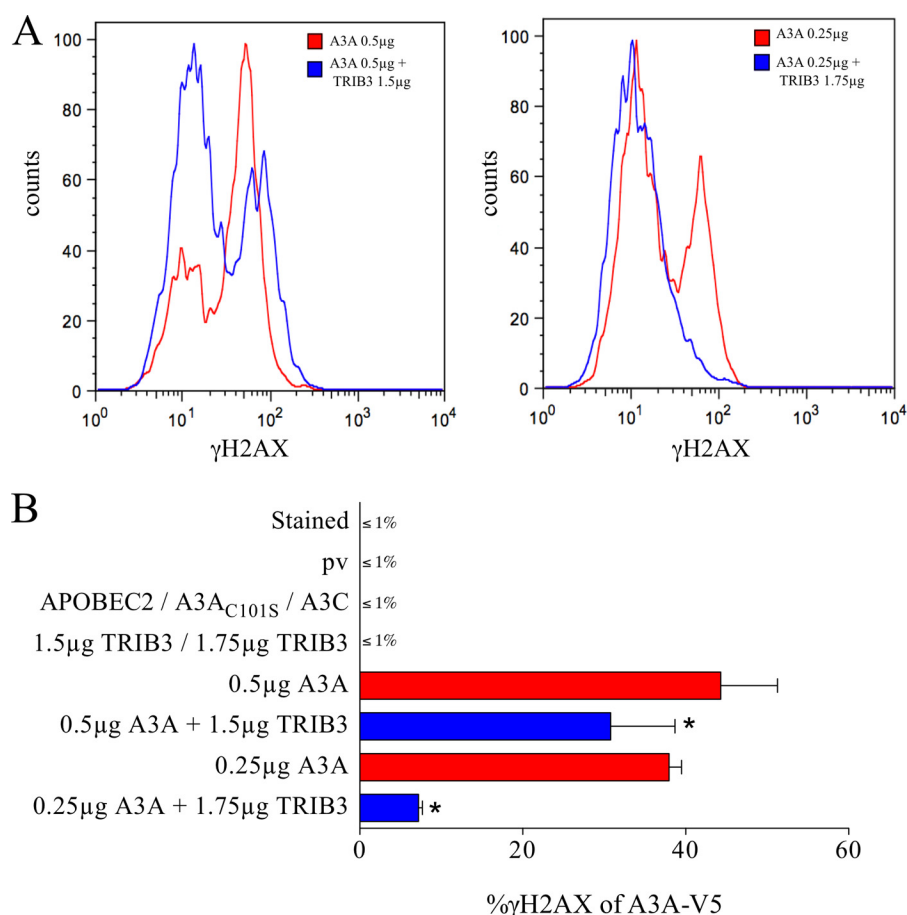


FIGURE 6. **A3A-induced DSBs can be countered by TRIB3.** *A*, superposition of FACS analysis of  $\gamma$ H2AX-positive HeLa cells gated on the V5-tagged A3A with and without TRIB3 at two different A3A:TRIB3 ratios. *B*, means and standard deviations  $\gamma$ H2AX-positive cell frequencies for quadruplicate transfections, DNA concentrations were always 2  $\mu$ g and compensated for by plasmid vector. \* indicates a statistically significant difference between two observed percentages ( $p < 0.05$ ).

**Relative A3A and TRIB3 Expression Levels**—To appreciate the relative expression levels of A3A and TRIB3, a TaqMan transcriptional study was made of A3 and TRIB3 genes using the *RPL13A* gene as reference (25, 26). In four established cell lines A3A levels were essentially zero excluding any meaningful comparison. Those for A3C were always  $>$ TRIB3 (supplemental Fig. S2D). In two donors, activated human PBMCs IFN $\alpha$  treatment up-regulated A3A (Fig. 7A) as previously noted (24–26). However, TRIB3 levels always exceeded those of A3A. The striking loss of A3A levels over time could reflect the loss of polymorphonuclear and myeloid cells which invariably express high levels of A3A rather than specific down-regulation of the gene. By contrast, in purified CD4 $^{+}$  T cells from two donors, gene levels were far more stable, and once again TRIB3 levels always exceeded those of A3A (Fig. 7B). To prove that A3A/TRIB3 interaction is physiological, we immunoprecipitated TRIB3 from human neutrophils isolated from peripheral blood of healthy donors, and A3A was detected with anti-A3A antibody. As control, anti-TRIB3 was also detected from the same complex (supplemental Fig. S3G). Hence, A3A/TRIB3 detection in neutrophil granulocytes suggests that this endogenous interaction is physiologically relevant (supplemental Fig. S3G).

To compare the A3A, A3C, and TRIB1–3 expression in inflamed tissue, a TaqMan PCR chip was performed on 41 cir-

rhotic samples and was compared with 4 healthy livers (17). The *RPL13A* gene was used as reference. Fig. 7C provides the TRIB1, TRIB2, and TRIB3 transcriptomes along with those for A3A and A3C. Although A3C was strongly up-regulated, there were few overall changes in any of the three Tribbles gene levels (Fig. 7D). When the A3A and TRIB3 levels were analyzed for individual samples, TRIB3 levels were always greater than those of A3A (Fig. 7D inset).

## DISCUSSION

TRIB3 was identified as an interactor for both A3A and A3C. Given that A3A alone of all A3 enzymes can edit nuclear DNA (28), we concentrated on the A3A/TRIB3 interaction and its consequences. TRIB3, which is essentially nuclear, effectively prevents A3A from editing nuDNA, essentially mopping up A3A being translocated to the nucleus, so protecting the genome. Nonetheless, some editing occurs when A3A is over-expressed as revealed by using the HEK-293-UGI cell line or co-transfection with siTRIB3. This suggests that A3A editing of nuDNA depends to some extent on the relative levels of A3A and TRIB3. In established cell lines, A3A levels are very low indeed whereas TRIB3 levels are comparable with those in some *in vivo* settings. A3A gene expression can be up-regulated by phorbol esters, poly(I:C), and interferon (24–26). In turn, TRIB3 is induced by endoplasmic reticulum stress (55) whereas



vation that high level, constitutively expressing A3A cell lines have not been obtained.

TRIB3 interacts with a wide variety of proteins, the majority being connected with DNA repair, or coupled to proteins linked to the maintenance of DNA stability and DNA repair (40). For example, TRIB3 is a G<sub>1</sub>/S and G<sub>2</sub>/M checkpoint protein (42, 43). Several studies have pointed to a role for *TRIB3* in human cancer to the point that it is considered as a tumor susceptibility gene. Importantly, TRIB3 interacts with CtIP, a nuclear cofactor of the transcriptional repressor CtBP (59). CtIP interacts with tumor suppressors such as the Rb family members and BRCA1 through binding sites that are frequently mutated in human cancers (60). In short, TRIB3 is part of the broad CtIP-Rb-BRCA1-ATM protein network that involves cell cycle control, cell survival, DNA repair, and genome stability. Finally the mixed lineage kinase MLK3 has been shown to interact with TRIB3, and attenuation of either compromised mitochondrial integrity and suppressed cellular survival mechanisms via TRB3-dependent inhibition of Akt (61). Three nonsense polymorphisms of TRIB3 have been noted, namely T27stop, Q40stop, and Q84stop, all mapping to the amino-terminal pseudo-NADPH-binding domain (supplemental Fig. S1B). So far there are no reports of *TRIB3*<sup>-/-</sup> or *TRIB3*<sup>+/-</sup> associated with cancer, but any depletion of *TRIB3* levels could increase albeit slightly the frequency of nuDNA hypoediting. In conclusion, through its control of APOBEC3A the present findings identify TRIB3 as another guardian of genome integrity.

*Acknowledgments*—We thank Drs. Endre Kiss-Toth for human *TRIB1* and 2 and murine *TRIB3* plasmids, Emmanuel Birlouez for three APOBEC3 plasmids, and Agnès Marchio for formatting Fig. 7C.

## REFERENCES

- Di Noia, J. M., and Neuberger, M. S. (2007) Molecular mechanisms of antibody somatic hypermutation. *Annu. Rev. Biochem.* **76**, 1–22
- Jarmuz, A., Chester, A., Bayliss, J., Gisbourne, J., Dunham, I., Scott, J., and Navaratnam, N. (2002) An anthropoid-specific locus of orphan C to U RNA-editing enzymes on chromosome 22. *Genomics* **79**, 285–296
- Harris, R. S., Bishop, K. N., Sheehy, A. M., Craig, H. M., Petersen-Mahrt, S. K., Watt, I. N., Neuberger, M. S., and Malim, M. H. (2003) DNA deamination mediates innate immunity to retroviral infection. *Cell* **113**, 803–809
- Lecossier, D., Bouchonnet, F., Clavel, F., and Hance, A. J. (2003) Hypermutation of HIV-1 DNA in the absence of the Vif protein. *Science* **300**, 1112
- Mangeat, B., Turelli, P., Caron, G., Friedli, M., Perrin, L., and Trono, D. (2003) Broad antiretroviral defense by human APOBEC3G through lethal editing of nascent reverse transcripts. *Nature* **424**, 99–103
- Mariani, R., Chen, D., Schräfelbauer, B., Navarro, F., König, R., Bollman, B., Münk, C., Nymark-McMahon, H., and Landau, N. R. (2003) Species-specific exclusion of APOBEC3G from HIV-1 virions by Vif. *Cell* **114**, 21–31
- Zhang, H., Yang, B., Pomerantz, R. J., Zhang, C., Arunachalam, S. C., and Gao, L. (2003) The cytidine deaminase CEM15 induces hypermutation in newly synthesized HIV-1 DNA. *Nature* **424**, 94–98
- Sheehy, A. M., Gaddis, N. C., Choi, J. D., and Malim, M. H. (2002) Isolation of a human gene that inhibits HIV-1 infection and is suppressed by the viral Vif protein. *Nature* **418**, 646–650
- Wiegand, H. L., Doehle, B. P., Bogerd, H. P., and Cullen, B. R. (2004) A second human antiretroviral factor, APOBEC3F, is suppressed by the HIV-1 and HIV-2 Vif proteins. *EMBO J.* **23**, 2451–2458
- Zheng, Y. H., Irwin, D., Kurosu, T., Tokunaga, K., Sata, T., and Peterlin, B. M. (2004) Human APOBEC3F is another host factor that blocks human immunodeficiency virus type 1 replication. *J. Virol.* **78**, 6073–6076
- Hultquist, J. F., Lengyel, J. A., Refsland, E. W., LaRue, R. S., Lackey, L., Brown, W. L., and Harris, R. S. (2011) Human and rhesus APOBEC3D, APOBEC3F, APOBEC3G, and APOBEC3H demonstrate a conserved capacity to restrict Vif-deficient HIV-1. *J. Virol.* **85**, 11220–11234
- Refsland, E. W., Hultquist, J. F., and Harris, R. S. (2012) Endogenous origins of HIV-1 G-to-A hypermutation and restriction in the nonpermissive T cell line CEM2n. *PLoS Pathog.* **8**, e1002800
- Noguchi, C., Ishino, H., Tsuge, M., Fujimoto, Y., Imamura, M., Takahashi, S., and Chayama, K. (2005) G to A hypermutation of hepatitis B virus. *Hepatology* **41**, 626–633
- Rösler, C., Köck, J., Kann, M., Malim, M. H., Blum, H. E., Baumert, T. F., and von Weizsäcker, F. (2005) APOBEC-mediated interference with hepadnavirus production. *Hepatology* **42**, 301–309
- Suspène, R., Guétard, D., Henry, M., Sommer, P., Wain-Hobson, S., and Vartanian, J. P. (2005) Extensive editing of both hepatitis B virus DNA strands by APOBEC3 cytidine deaminases *in vitro* and *in vivo*. *Proc. Natl. Acad. Sci. U.S.A.* **102**, 8321–8326
- Turelli, P., Mangeat, B., Jost, S., Vianin, S., and Trono, D. (2004) Inhibition of hepatitis B virus replication by APOBEC3G. *Science* **303**, 1829
- Vartanian, J. P., Henry, M., Marchio, A., Suspène, R., Aynaud, M. M., Guétard, D., Cervantes-Gonzalez, M., Battiston, C., Mazzaferro, V., Pineau, P., Dejean, A., and Wain-Hobson, S. (2010) Massive APOBEC3 editing of hepatitis B viral DNA in cirrhosis. *PLoS Pathog.* **6**, e1000928
- Vartanian, J. P., Guétard, D., Henry, M., and Wain-Hobson, S. (2008) Evidence for editing of human papillomavirus DNA by APOBEC3 in benign and precancerous lesions. *Science* **320**, 230–233
- Suspène, R., Aynaud, M. M., Koch, S., Pasdeloup, D., Labetoulle, M., Gaertner, B., Vartanian, J. P., Meyerhans, A., and Wain-Hobson, S. (2011) Genetic editing of herpes simplex virus 1 and Epstein-Barr herpesvirus genomes by human APOBEC3 cytidine deaminases in culture and *in vivo*. *J. Virol.* **85**, 7594–7602
- Tsuge, M., Noguchi, C., Akiyama, R., Matsushita, M., Kunihiro, K., Tanaka, S., Abe, H., Mitsui, F., Kitamura, S., Hatakeyama, T., Kimura, T., Miki, D., Hiraga, N., Imamura, M., Takahashi, S., Hayses, C. N., and Chayama, K. (2010) G to A hypermutation of TT virus. *Virus Res.* **149**, 211–216
- Bulliard, Y., Narvaiza, I., Bertero, A., Peddi, S., Röhrig, U. F., Ortiz, M., Zoete, V., Castro-Díaz, N., Turelli, P., Telenti, A., Michielin, O., Weitzman, M. D., and Trono, D. (2011) Structure-function analyses point to a polynucleotide-accommodating groove essential for APOBEC3A restriction activities. *J. Virol.* **85**, 1765–1776
- Chen, H., Lilley, C. E., Yu, Q., Lee, D. V., Chou, J., Narvaiza, I., Landau, N. R., and Weitzman, M. D. (2006) APOBEC3A is a potent inhibitor of adeno-associated virus and retrotransposons. *Curr. Biol.* **16**, 480–485
- Bonvin, M., Achermann, F., Greeve, I., Stroka, D., Keogh, A., Inderbitzin, D., Candinas, D., Sommer, P., Wain-Hobson, S., Vartanian, J. P., and Greeve, J. (2006) Interferon-inducible expression of APOBEC3 editing enzymes in human hepatocytes and inhibition of hepatitis B virus replication. *Hepatology* **43**, 1364–1374
- Koning, F. A., Newman, E. N., Kim, E. Y., Kunstman, K. J., Wolinsky, S. M., and Malim, M. H. (2009) Defining APOBEC3 expression patterns in human tissues and hematopoietic cell subsets. *J. Virol.* **83**, 9474–9485
- Refsland, E. W., Stenglein, M. D., Shindo, K., Albin, J. S., Brown, W. L., and Harris, R. S. (2010) Quantitative profiling of the full APOBEC3 mRNA repertoire in lymphocytes and tissues: implications for HIV-1 restriction. *Nucleic Acids Res.* **38**, 4274–4284
- Stenglein, M. D., Burns, M. B., Li, M., Lengyel, J., and Harris, R. S. (2010) APOBEC3 proteins mediate the clearance of foreign DNA from human cells. *Nat. Struct. Mol. Biol.* **17**, 222–229
- Landry, S., Narvaiza, I., Linfesty, D. C., and Weitzman, M. D. (2011) APOBEC3A can activate the DNA damage response and cause cell cycle arrest. *EMBO Rep.* **12**, 444–450
- Suspène, R., Aynaud, M. M., Guétard, D., Henry, M., Eckhoff, G., Marchio, A., Pineau, P., Dejean, A., Vartanian, J. P., and Wain-Hobson, S. (2011) Somatic hypermutation of human mitochondrial and nuclear DNA by

## Tribbles 3 Protects Nuclear DNA from APOBEC3A

- APOBEC3 cytidine deaminases, a pathway for DNA catabolism. *Proc. Natl. Acad. Sci. U.S.A.* **108**, 4858–4863
29. Bross, L., Muramatsu, M., Kinoshita, K., Honjo, T., and Jacobs, H. (2002) DNA double-strand breaks: prior to but not sufficient in targeting hypermutation. *J. Exp. Med.* **195**, 1187–1192
30. Conticello, S. G., Ganesh, K., Xue, K., Lu, M., Rada, C., and Neuberger, M. S. (2008) Interaction between antibody-diversification enzyme AID and spliceosome-associated factor CTNNB1. *Mol. Cell* **31**, 474–484
31. Ta, V. T., Nagaoka, H., Catalan, N., Durandy, A., Fischer, A., Imai, K., Nonoyama, S., Tashiro, J., Ikegawa, M., Ito, S., Kinoshita, K., Muramatsu, M., and Honjo, T. (2003) AID mutant analyses indicate requirement for class-switch-specific cofactors. *Nat. Immunol.* **4**, 843–848
32. Kou, T., Marusawa, H., Kinoshita, K., Endo, Y., Okazaki, I. M., Ueda, Y., Kodama, Y., Haga, H., Ikai, I., and Chiba, T. (2007) Expression of activation-induced cytidine deaminase in human hepatocytes during hepatocarcinogenesis. *Int. J. Cancer* **120**, 469–476
33. Komori, J., Marusawa, H., Machimoto, T., Endo, Y., Kinoshita, K., Kou, T., Haga, H., Ikai, I., Uemoto, S., and Chiba, T. (2008) Activation-induced cytidine deaminase links bile duct inflammation to human cholangiocarcinoma. *Hepatology* **47**, 888–896
34. Matsumoto, Y., Marusawa, H., Kinoshita, K., Endo, Y., Kou, T., Morisawa, T., Azuma, T., Okazaki, I. M., Honjo, T., and Chiba, T. (2007) *Helicobacter pylori* infection triggers aberrant expression of activation-induced cytidine deaminase in gastric epithelium. *Nat. Med.* **13**, 470–476
35. Okazaki, I. M., Hiai, H., Kakazu, N., Yamada, S., Muramatsu, M., Kinoshita, K., and Honjo, T. (2003) Constitutive expression of AID leads to tumorigenesis. *J. Exp. Med.* **197**, 1173–1181
36. Takai, A., Toyoshima, T., Uemura, M., Kitawaki, Y., Marusawa, H., Hiai, H., Yamada, S., Okazaki, I. M., Honjo, T., Chiba, T., and Kinoshita, K. (2009) A novel mouse model of hepatocarcinogenesis triggered by AID-causing deleterious p53 mutations. *Oncogene* **28**, 469–478
37. Yamanaka, S., Balestra, M. E., Ferrell, L. D., Fan, J., Arnold, K. S., Taylor, S., Taylor, J. M., and Innerarity, T. L. (1995) Apolipoprotein B mRNA-editing protein induces hepatocellular carcinoma and dysplasia in transgenic animals. *Proc. Natl. Acad. Sci. U.S.A.* **92**, 8483–8487
38. Gallois-Montbrun, S., Kramer, B., Swanson, C. M., Byers, H., Lynham, S., Ward, M., and Malim, M. H. (2007) Antiviral protein APOBEC3G localizes to ribonucleoprotein complexes found in P bodies and stress granules. *J. Virol.* **81**, 2165–2178
39. Mayumi-Matsuda, K., Kojima, S., Suzuki, H., and Sakata, T. (1999) Identification of a novel kinase-like gene induced during neuronal cell death. *Biochem. Biophys. Res. Commun.* **258**, 260–264
40. Hegedus, Z., Czibula, A., and Kiss-Toth, E. (2007) Tribbles: a family of kinase-like proteins with potent signaling regulatory function. *Cell. Signal.* **19**, 238–250
41. Du, K., Herzig, S., Kulkarni, R. N., and Montminy, M. (2003) TRB3: a Tribbles homolog that inhibits Akt/PKB activation by insulin in liver. *Science* **300**, 1574–1577
42. Kiss-Toth, E., Bagstaff, S. M., Sung, H. Y., Jozsa, V., Dempsey, C., Caunt, J. C., Oxley, K. M., Wyllie, D. H., Polgar, T., Harte, M., O'Neill, L. A., Qvarnstrom, E. E., and Dower, S. K. (2004) Human Tribbles, a protein family controlling mitogen-activated protein kinase cascades. *J. Biol. Chem.* **279**, 42703–42708
43. Sakai, S., Ohoka, N., Onozaki, K., Kitagawa, M., Nakanishi, M., and Hayashi, H. (2010) Dual mode of regulation of cell division cycle 25 A protein by TRB3. *Biol. Pharm. Bull.* **33**, 1112–1116
44. Walhout, A. J., and Vidal, M. (2001) High-throughput yeast two-hybrid assays for large-scale protein interaction mapping. *Methods* **24**, 297–306
45. Mendoza, J. A., Jacob, Y., Cassonnet, P., and Favre, M. (2006) Human papillomavirus type 5 E6 oncoprotein represses the transforming growth factor  $\beta$  signaling pathway by binding to SMAD3. *J. Virol.* **80**, 12420–12424
46. Suspène, R., Henry, M., Guillot, S., Wain-Hobson, S., and Vartanian, J. P. (2005) Recovery of APOBEC3-edited human immunodeficiency virus G  $\rightarrow$  A hypermutants by differential DNA denaturation PCR. *J. Gen. Virol.* **86**, 125–129
47. Wang, Z., and Mosbaugh, D. W. (1988) Uracil-DNA glycosylase inhibitor of bacteriophage PBS2: cloning and effects of expression of the inhibitor gene in *Escherichia coli*. *J. Bacteriol.* **170**, 1082–1091
48. Bogerd, H. P., Wiegand, H. L., Hulme, A. E., Garcia-Perez, J. L., O'Shea, K. S., Moran, J. V., and Cullen, B. R. (2006) Cellular inhibitors of long interspersed element 1 and Alu retrotransposition. *Proc. Natl. Acad. Sci. U.S.A.* **103**, 8780–8785
49. Yacoub Wasef, S. Z., Robinson, K. A., Berkaw, M. N., and Buse, M. G. (2006) Glucose, dexamethasone, and the unfolded protein response regulate TRB3 mRNA expression in 3T3-L1 adipocytes and L6 myotubes. *Am. J. Physiol. Endocrinol. Metab.* **291**, E1274–E1280
50. Berger, G., Durand, S., Fargier, G., Nguyen, X. N., Cordeil, S., Bouaziz, S., Muriaux, D., Darlix, J. L., and Cimarelli, A. (2011) APOBEC3A is a specific inhibitor of the early phases of HIV-1 infection in myeloid cells. *PLoS Pathog.* **7**, e1002221
51. Schrader, C. E., Linehan, E. K., Mochevova, S. N., Woodland, R. T., and Stavnezer, J. (2005) Inducible DNA breaks in Ig S regions are dependent on AID and UNG. *J. Exp. Med.* **202**, 561–568
52. Chiarle, R., Zhang, Y., Frock, R. L., Lewis, S. M., Molin, B., Ho, Y. J., Myers, D. R., Choi, V. W., Compagno, M., Malkin, D. J., Neuber, D., Monti, S., Giallourakis, C. C., Gostissa, M., and Alt, F. W. (2011) Genome-wide translocation sequencing reveals mechanisms of chromosome breaks and rearrangements in B cells. *Cell* **147**, 107–119
53. Hasham, M. G., Donghia, N. M., Coffey, E., Maynard, J., Snow, K. J., Ames, J., Wilpan, R. Y., He, Y., King, B. L., and Mills, K. D. (2010) Widespread genomic breaks generated by activation-induced cytidine deaminase are prevented by homologous recombination. *Nat. Immunol.* **11**, 820–826
54. Rogakou, E. P., Pilch, D. R., Orr, A. H., Ivanova, V. S., and Bonner, W. M. (1998) DNA double-stranded breaks induce histone H2AX phosphorylation on serine 139. *J. Biol. Chem.* **273**, 5858–5868
55. Ohoka, N., Yoshii, S., Hattori, T., Onozaki, K., and Hayashi, H. (2005) TRB3, a novel ER stress-inducible gene, is induced via ATF4-CHOP pathway and is involved in cell death. *EMBO J.* **24**, 1243–1255
56. Smith, S. M., Moran, A. P., Duggan, S. P., Ahmed, S. E., Mohamed, A. S., Windle, H. J., O'Neill, L. A., and Kelleher, D. P. (2011) Tribbles 3: a novel regulator of TLR2-mediated signaling in response to *Helicobacter pylori* lipopolysaccharide. *J. Immunol.* **186**, 2462–2471
57. Johnson, J. A., Carstensen, B., Witte, D., Bowker, S. L., Lipscombe, L., and Renehan, A. G. (2012) Diabetes and cancer. 1. Evaluating the temporal relationship between type 2 diabetes and cancer incidence. *Diabetologia* **55**, 1607–1618
58. Renehan, A. G., Yeh, H. C., Johnson, J. A., Wild, S. H., Gale, E. A., Möller, H., and Diabetes and Cancer Research Consortium (2012) Diabetes and cancer. 2. Evaluating the impact of diabetes on mortality in patients with cancer. *Diabetologia* **55**, 1619–1632
59. Xu, J., Lv, S., Qin, Y., Shu, F., Xu, Y., Chen, J., Xu, B. E., Sun, X., and Wu, J. (2007) TRB3 interacts with CtIP and is overexpressed in certain cancers. *Biochim. Biophys. Acta* **1770**, 273–278
60. Chinnadurai, G. (2006) CtIP, a candidate tumor susceptibility gene, is a team player with luminaries. *Biochim. Biophys. Acta* **1765**, 67–73
61. Humphrey, R. K., Newcomb, C. J., Yu, S. M., Hao, E., Yu, D., Krajewski, S., Du, K., and Jhala, U. S. (2010) Mixed lineage kinase-3 stabilizes and functionally cooperates with TRIBBLES-3 to compromise mitochondrial integrity in cytokine-induced death of pancreatic  $\beta$  cells. *J. Biol. Chem.* **285**, 22426–22436